

Interfacial changes of optical fibers in the cementitious environment

C. K. Y. LEUNG, D. DARMAWANGSA

Department of Civil Engineering, Hong Kong University of Science and Technology,
Clear Water Bay, Kowloon, Hong Kong

E-mail: ckleung@usthk.ust.hk

Embedded optical fiber sensors have recently been employed for strain and crack monitoring in concrete structures. The performance of the sensor is strongly affected by the fiber/matrix interface. For strain monitoring, effective stress transfer between fiber and matrix is required. A high interfacial bond is therefore desirable. On the other hand, crack sensing may rely on fiber debonding and bending, which is only possible with a weak interfacial bond. In the cementitious environment, the interfacial properties are known to vary with time, and this may affect the long-term performance of embedded optical sensors. The objective of the present investigation is to study the interfacial changes when specimens containing embedded optical fibers (with different coatings) are subject to different environmental conditions including wet curing, wetting/drying and freezing/thawing. Fibers removed from the matrix are examined under the SEM. Also, fiber pull-out specimens are prepared and tested. The results show that the fiber pull-out test can reveal significant changes in interfacial behaviour that cannot be detected from SEM examination. The pull-out test is therefore demonstrated to be a useful technique for the characterization of time dependent interfacial behavior for embedded optical fiber sensors. © 2000 Kluwer Academic Publishers

1. Introduction

Concrete is the most widely used structural material in construction. Its long-term degradation is a major problem with the infrastructure of many developed countries. Damage in a concrete structure may start very early in its life span. For example, in large structures such as dams, the high thermal gradients that exist during the initial curing process may lead to cracking. Such thermal cracking can be avoided through feedback control, provided small strain changes of below $10 \mu\epsilon$ can be measured [1]. In the long run, loading/environmental effects can also result in severe degradation. Highway bridges under heavy traffic and freezing/thawing are familiar examples. To properly maintain concrete structures in order to extend their service life, it is highly desirable to develop sensors that can monitor structural condition throughout its life span.

Optical fiber sensors have recently been embedded in various concrete structures such as buildings [1, 2], dams [3] and bridges [4, 5] to monitor strain in the structure. Their high resolution (below $1 \mu\epsilon$ with interferometric techniques) makes them ideal sensors for control applications. Also, since light signal rather than electric current is carried, optical fiber sensors have very little losses and are immune to electromagnetic interference and lightning damages. For large structures in open areas (e.g. dams and bridges), or those carrying power lines (such as bridges with power lines underneath), optical fiber sensors appear to be ideal.

The long-term durability of optical fiber sensors in the concrete environment is an issue of major concern. Durability problems can arise from two different sources. First, when cement is mixed with water, the hydration reactions produce calcium silicate hydrate, a gel-like microstructure giving strength to concrete, and calcium hydroxide, which gives rise to an alkaline environment in concrete. In all commercial optical fibers, a polymeric coating is applied to protect the fiber from surface scratches and environmental attack. Once the coating deteriorates, hydroxide ions can diffuse to the glass surface and induce corrosion. The second cause of durability problems, which is not as obvious as the first, is related to the changes at the fiber/matrix interface. The performance of optical sensor is affected by the interfacial bonding between the fiber and the matrix. When sensors are used for the measurement of tensile strain, the interfacial stresses are responsible for strain transfer between the concrete and the fiber. Deterioration of interfacial bond may lead to ineffective transfer that affects the calibration of the optical sensor. On the other hand, Leung *et al.* [6] have recently developed a crack sensor based on the monitoring of fiber bending loss as cracks open in a concrete structure (Note: see section 3.2 for more details). For the fiber to bend, it has to first debond from the concrete and slide. If the interfacial bond is too high, crack opening may lead to fiber breakage instead. For the crack sensor, an increase in interfacial bonding with

time is therefore not desirable. In the cementitious environment, the properties at the fiber/matrix interface have been found to vary with time [7]. Such variations may affect the performance of the optical fiber sensor.

This investigation will focus on the second cause of durability problems related to the change in interfacial properties. In the literature, two related pieces of work can be found. In Habel and Polster [8], fibers of various coatings (polyimide, acrylate and fluorine thermoplastic) are embedded in mortar blocks and removed after a given period of time for SEM (Scanning Electron Microscope) examination. Any degradation of the coating can hence be visually observed. In their work, besides visible damages, other plausible changes in interfacial bonding condition cannot be determined. Also, all the specimens are subject to wet curing. In real structures, the embedded fiber may be under severe environmental conditions such as freezing/thawing and wetting/drying. Such effects have not been considered in [8]. In Escobar *et al.* [9], optical fiber sensors with a teftzel silicone coating are embedded in concrete for five years and tested. The obtained results are the same as those in a short-term test. This work establishes the fact that the silicone coating is effective in protecting the glass fiber and the interface allows effective stress transfer after five years. However, it is not clear if the interfacial bond may become excessively strong for crack sensing applications. Also, the effect of exposure conditions such as freezing/thawing and wetting/drying has not been studied.

In the present investigation, fibers of three different coatings (acrylate, polyimide/hytreil and teftzel-silicone) are embedded in mortar specimens and subject to various environmental conditions. SEM studies are carried out to observe the surface deterioration. Also, a fiber pull-out testing procedure is developed to measure the interfacial bonding/slipping behavior and to study the effect of aging (under different environments) on such behavior. Test results up to about three months are reported. Our result indicates that the fiber pull-out test can reveal information not obtainable from SEM examination. The present investigation therefore establishes the fiber pull-out test as an effective means to assess interfacial changes (and hence, the long-term behavior) of embedded optical fiber sensors.

2. Experimental program

2.1. Material and specimen preparation for the testing

Optical fibers with three different coatings are studied in this work. These include:

- (1) Acrylate-coated fibers (glass diameter = $125 \mu\text{m}$, total diameter = $250 \pm 20 \mu\text{m}$)
- (2) Polyimide/Hytreil coated fibers (glass diameter = $100 \mu\text{m}$, polyimide diameter = $139 \mu\text{m}$, total diameter = $400 \pm 30 \mu\text{m}$)
- (3) Teftzel-silicone-coated fibers (glass diameter = $104 \mu\text{m}$, total diameter = $120 \pm 7 \mu\text{m}$)

It should be noted that the total diameter includes the glass fiber and its coating. The acrylate coated fiber

is fabricated at the Lightwave Technology Laboratory of Brown University, while the other two fibers are provided by Polymicro Technologies. For the polyimide/hytreil fiber, the coating is of the composite type, with a thin layer of polyimide surrounded by a much thicker layer of hytreil. For the other two fibers, the coating is made of a single material.

Specimens for both the SEM investigation and fiber pull-out test are prepared with sand, water and type III portland cement. The sand is sifted to pass through a number 25 sieve ($600 \mu\text{m}$), while the cement passes through a number 200 sieve ($75 \mu\text{m}$). A water : cement : sand ratio of 0.5 : 1 : 2 is employed. To prepare specimens, the mortar is mixed in a Kitchen Aid K5SS mixer. The cement and sand are first blended for 3 minutes. One third of the water is then added, followed by two minutes of further mixing. The process is repeated until all the water is put in.

After mixing, the mortar is placed into molds to make specimens. For both SEM investigation and fiber pull-out test, a mold of internal dimension $25.4 \text{ mm} \times 25.4 \text{ mm} \times 9.5 \text{ mm}$ thick is employed. For SEM specimens, two holes are drilled at opposite sides of the mold for an optical fiber to pass through at mid-height. The length of embedded fiber in the specimen is hence 25.4 mm . To facilitate specimen removal, releasing oil is sprayed on the internal surfaces of the mold. After the fiber is placed and mortar is added, a razor blade (covered with releasing oil) is embedded in close proximity to the fiber, but with extreme care to avoid contact. The specimens are kept moist by covering with plastic wrap. After 24 hours, they are removed from the mold and the razor blades are carefully extracted. The specimens are then put into a water bath for further curing. The groove left behind by the razor blade will facilitate the breaking of specimen to extract the embedded fiber for SEM study. Note that this approach is similar to that adopted by Habel and Polster [8].

The preparation of pull-out specimens is illustrated in Fig. 1. A length of optical fiber is first inserted into a small hole in a PMMA block. A free length of 10 mm is left outside the block. To secure the fiber, a small amount of clay is added to the hole. Blocks with the fiber are then placed into matching molds (see Fig. 1). Releasing oil is applied to all internal surfaces, with special care taken to avoid contaminating the fiber. Mortar is then cast to make a pull-out specimen of size

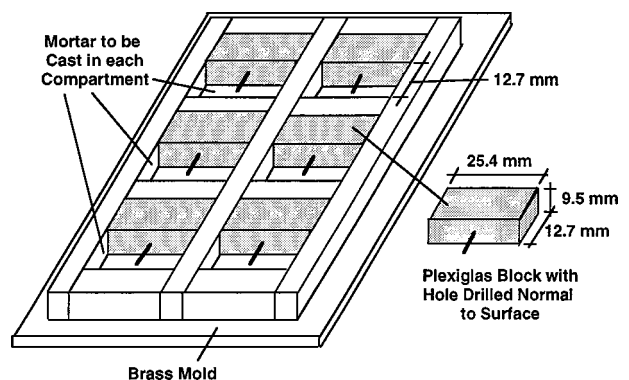


Figure 1 Mold for making fiber pull-out specimens.

25.4 mm × 12.7 mm × 9.5 mm. After casting, the mold is covered with plastic wrap for 24 hours. The specimens are then removed and placed in the water bath.

To study the effects of environmental exposure, the specimens are subject to the following conditions before SEM investigation and pull-out testing.

(i) Specimens with embedded fibers are left in a water bath for different periods of time (1 week, 2 weeks, 3 weeks, 1 month and 3 months) before testing. The purpose of this series of test is to investigate the effect of cementitious environment on the fiber.

(ii) After curing for 14 days in the water bath, the specimens are subject to 30 or 60 cycles of freezing/thawing. Each freeze/thaw cycle involves 12 hours of freezing in the freezer and 12 hours of thawing under room temperature. After 30 and 60 freeze/thaw cycles, the specimen ages are 44 and 74 days respectively.

(iii) After curing for 14 days in the water bath, the specimens are subject to 20 or 40 cycles of wetting/drying. In each wetting/drying cycle, the specimen is kept in the water bath for 12 hours and then removed from water. After the surface is wiped dry, the specimens are kept in air for 12 hours before putting it back into the water bath. After 20 and 40 wetting/drying cycles, the specimen ages are 34 and 54 days respectively.

Since the specimen size is quite small, we believe 12 hours is sufficient for the whole specimen to experience significant changes in its temperature or moisture conditions.

Besides fibers embedded in mortar, durability studies are also carried out with bare fibers. Optical fibers are stored in (i) water, and (ii) calcium hydroxide solution with pH = 13. SEM examinations are carried out after 1 week, 2 weeks, 3 weeks, 1 month and 3 months. Surface conditions are compared with those for embedded fibers. If similar results are obtained, future durability tests can be carried out in water or alkaline solution. The trouble of embedding fibers into mortar specimens and subsequent removal for inspection can then be avoided.

2.2. Testing procedure for scanning electron microscopy

To carry out SEM examination of embedded fibers, the specimens are gripped tightly and bent to induce tension on the side with the groove (left by the razor blade). In most cases, the crack will propagate towards the fiber, exposing it while the specimen splits into two halves. The exposed fiber is then carefully removed from the specimen. With several specimens subject to each environmental condition, we are successful in exposing the fiber in at least one specimen per case. For SEM examination, the fibers are glued to metallic mounts and coated with a thin layer of gold. Careful attention is taken in handling the fiber to avoid the introduction of surface damages.

2.3. Testing procedure for fiber pull-out test

The fiber pull-out test is carried out in a set-up developed in our laboratory (Fig. 2). The pull-out specimen

is glued to a L-shape holder, with the fiber secured by a specially designed grip (to be described later). The grip is held by a hardened steel rod that passes through a ball-bearing block. On the other side of the rod is the load cell. The purpose of the ball-bearing block is to ensure linear movement of the rod during pull-out testing. The resistance offered by the bearing block can be measured by pulling the rod itself without the pull-out specimen. This resistance turns out to be very small and its value is subtracted from all measured loads during the pull-out test. On the other side of the load cell is a keyed rod that passes through a block with a key-way machined in close tolerance to the size of the key. The end of the keyed rod is screwed into a nut resting on a reaction block. Once the motor is started to turn the nut, linear motion of the rods (rather than rotation) will be introduced.

Due to the extreme brittleness and small size of the optical fibers, a special procedure needs to be developed for fiber gripping and alignment. The procedure we adopted is described below:

(i) The two sides of the pull-out specimen, which will be in contact with the L-shape holder, are first sanded to ensure proper attachment to the holder.

(ii) The acrylate and tefzel-silicone coated fibers have much lower coating thickness than the polyimide/hytre coated fiber. As a result, they break very easily if directly gripped. By wrapping two layers of thin tape around the fiber, a buffer is provided and the fibers become much less susceptible to breakage.

(iii) The fiber grip is shown in Fig. 3. It is a two-part grip with a small groove machined right between the upper and lower parts, at an angle perpendicular to

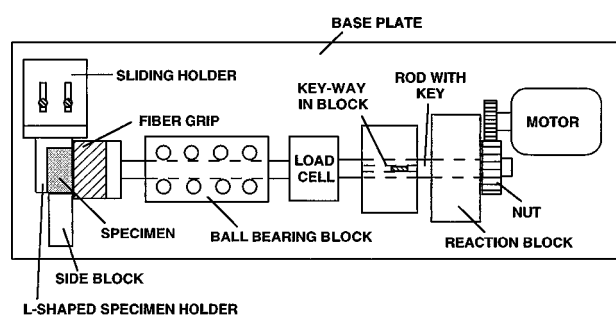


Figure 2 Equipment for the fiber pull-out test.

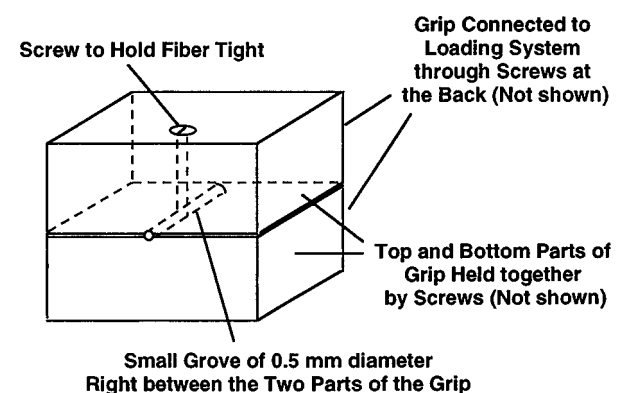


Figure 3 Split grip for the fiber pull-out test.

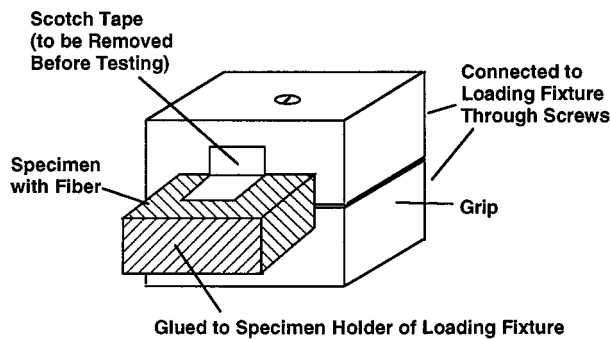


Figure 4 Fiber grip with the pull-out specimen.

the grip surface. After the fiber is placed into the groove, the two parts are screwed together and a third screw, which is right on top of the groove, can be tightened to secure the fiber. To prevent fiber bending at this stage, the pull-out specimen is pushed against the surface of the grip and taped to it (Fig. 4). This way, the specimen and grip behave as a 'single block' during the alignment procedure and no pre-mature fiber pulling or bending can occur.

(iv) To align the fiber in the loading system, the grip is first screwed to a plate at the end of the hardened steel rod. The L-shaped specimen holder is then attached to a movable steel angle (the sliding holder in Fig. 2). 5-minute epoxy is mixed and applied to surfaces of the pull-out specimen as well as the specimen holder.

(v) By moving both the hardened steel rod (with the grip) and the steel angle, the pull-out specimen and specimen holder are moved towards one another until the surfaces touch. The steel angle is then fixed in place (by tightening the screws on the sliding holder) and the system is left in this position for 30 minutes until the epoxy is sufficiently cured. With this alignment procedure, the fiber is already aligned in the grip before the specimen is glued to the holder. After the epoxy hard-

ens, no further adjustment is required. When loading is applied, the present set-up will theoretically produce bending and rotation of the specimen holder (since it is only supported on one side by the sliding steel angle). However, since the pull-out load is very small and the steel angle is quite stiff, this effect is negligible.

(vi) After the epoxy hardens, a LVDT holder is attached to the back of the specimen holder, and a target block is attached to the grip. A small LVDT is then employed to measure displacement during the pull-out test.

(vii) After everything is set up, the nut is engaged to the motor. Gear ratios are chosen in such a way that the displacement rate is $6.615 \mu\text{m/s}$. During testing, the output from both the load cell and LVDT are recorded by a computer through a data logger.

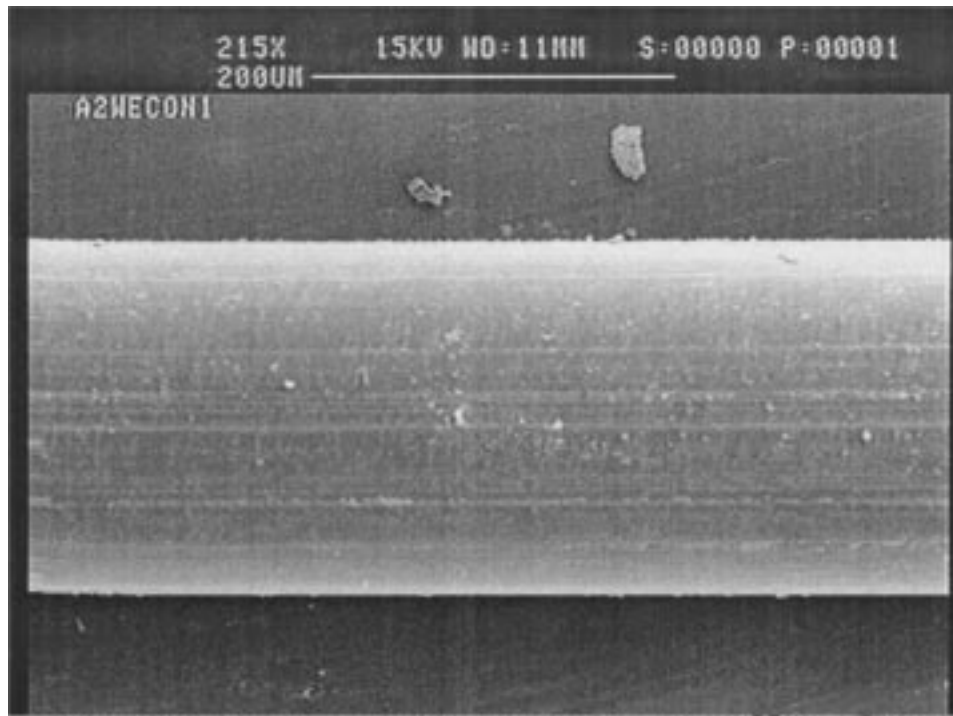
3. Results and discussions

3.1. Scanning electron microscopy (SEM) investigation of fiber surface

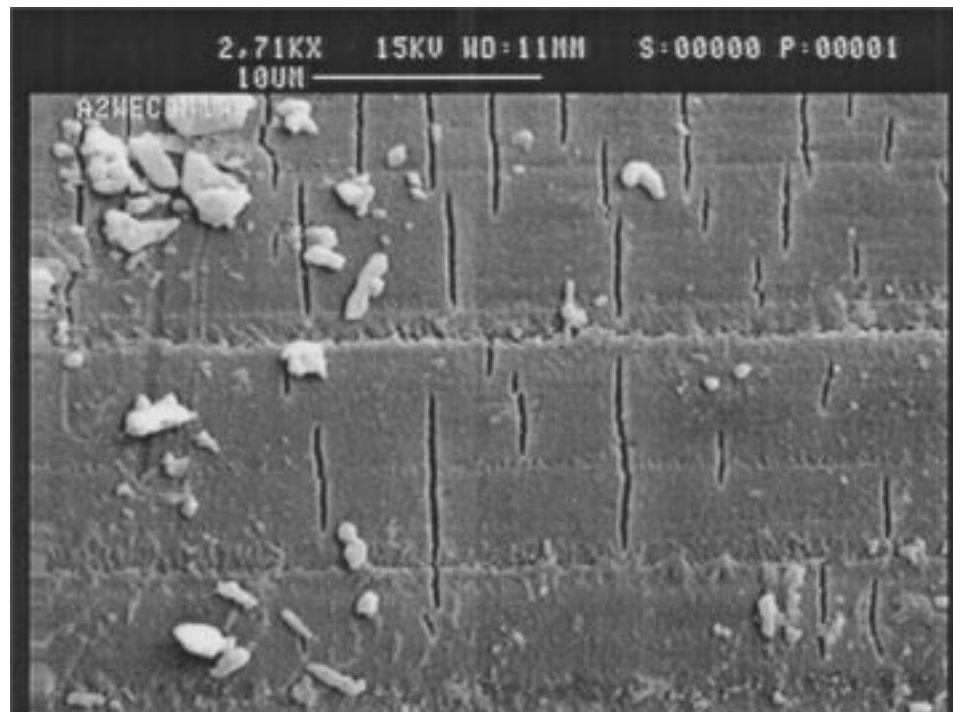
The result of the SEM investigation is summarized in Table I. For the polyimide/hytrel and tefzel-silicone coatings, regardless of the type of environmental exposure, no noticeable surface damage can be observed at about $3000\times$ magnification. For the acrylate coating, surface cracking can be observed in a number of cases, shown in Figs 5–10. Note that the micrographs for different cases may be shown at different degrees of magnification to clearly reveal the damages. When placed in water or calcium hydroxide solution, the acrylate coating shows no significant deterioration. Only after 3-month storage in water will thin hairline cracks be observable. However, if the fiber is embedded inside the mortar specimen, minor surface cracking starts to occur after 2 weeks, and becomes much more severe after one month. A plausible explanation is that minor surface damages can be introduced during the casting process no matter how much care has been taken. Such damages may couple with chemical effects,

TABLE I Summary of the SEM study

	Period	Acrylate	Polyimide/Hytrel	Teftzel-Silicone
Stored inside the Water Tank	1 week	Good	Good	Good
	2 weeks	Good	Good	Good
	3 weeks	Good	Good	Good
	1 month	Good	Good	Good
	3 months	Hairline Cracks	Good	Good
Stored in Calcium Hydroxide Solution (pH = 13.0)	Period	Acrylate	Polyimide/Hytrel	Teftzel-Silicone
	1 week	N/A	Good	Good
	2 weeks	N/A	Good	Good
	3 weeks	Good	Good	Good
	1 month	Good	Good	Good
Embedded inside Mortar Specimen	Period	Acrylate	Polyimide/Hytrel	Teftzel-Silicone
	2 weeks	Hairline Cracks	Good	Good
	1 month	Significant Cracking	Good	Good
	3 months	Severe Cracking	Good	Good
Wet-Dry Cycles	Cycles	Acrylate	Polyimide/Hytrel	Teftzel-Silicone
	20 cycles	Significant Cracking	Good	Good
	40 cycles	Severe Cracking	Good	Good
Freeze-Thaw Cycles	Cycles	Acrylate	Polyimide/Hytrel	Teftzel-Silicone
	30 cycles	Good	Good	Good
	60 cycles	Severe Cracking	Good	Good



(a)



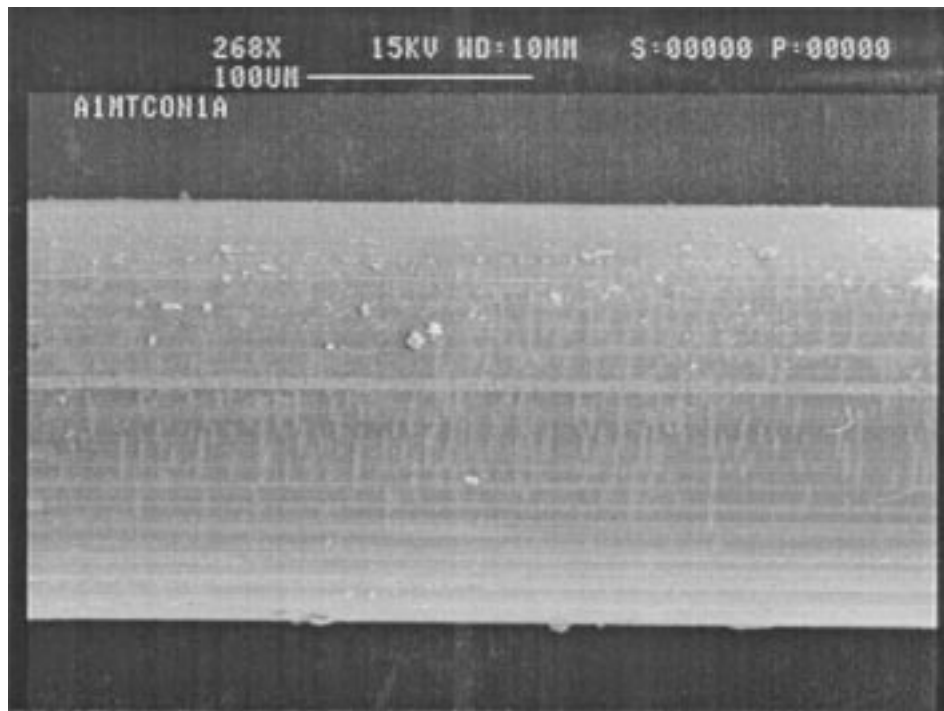
(b)

Figure 5 Acrylate-coated fiber in cement mortar for (a) two weeks (215 \times); (b) two weeks (2710 \times).

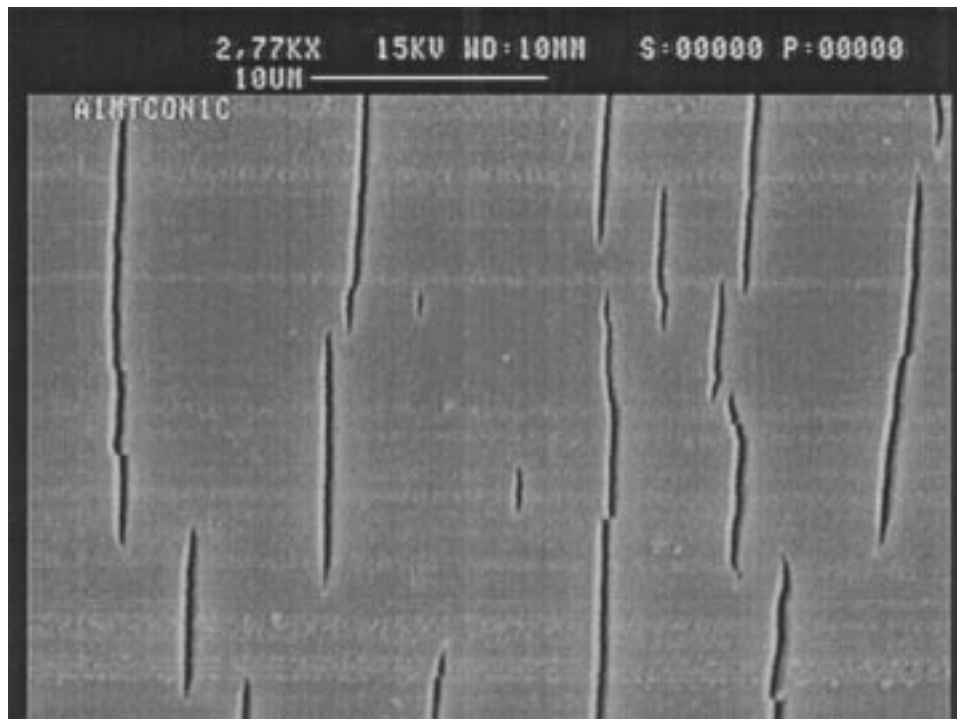
leading to more severe deterioration. The results indicate that it is important to carry out durability tests with optical fibers embedded in mortar specimens. Simply putting the fibers into water or alkaline solution is not appropriate.

Some interesting trends can be observed by comparing the micrographs for fibers embedded in mortar alone and those subject to freeze/thaw and wetting/drying cycles as well. After 20 wet/dry cycles (which is $14 + 20 = 34$ days of age), the degree of cracking (shown in Fig. 8) is clearly much more significant than that in a specimen of similar age (one month)

without going through the moisture cycling (Fig. 6). Repeated wetting/drying can therefore accelerate the deterioration of acrylate coating. However, after 30 cycles of freezing/thawing (44 days of age), no damage can be observed on the fiber surface, whereas cracking can be clearly seen after one month if there is no freeze/thaw cycling. It should be noted that in the freezing/thawing experiments, the specimen is left in air during the thawing stage. When the specimen is thawed, partial drying may occur due to evaporation of water. The specimen is then returned to the freezer for the freezing stage. The freeze/thaw cycles are therefore carried out with



(a)



(b)

Figure 6 Acrylate-coated fiber in cement mortar for (a) one month (268 \times); (b) one month (2770 \times).

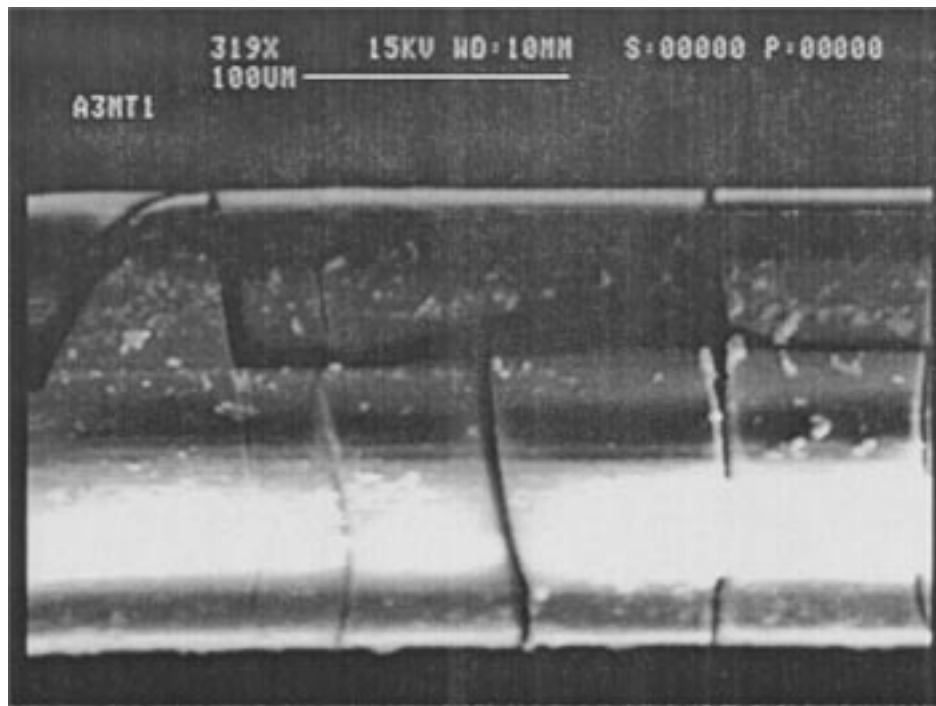
the moisture content gradually reduced. This may explain the deceleration of damage observed in our tests. In future experiments, it will be of interest to carry out thawing in water to clarify this issue.

3.2. Fiber pull-out test

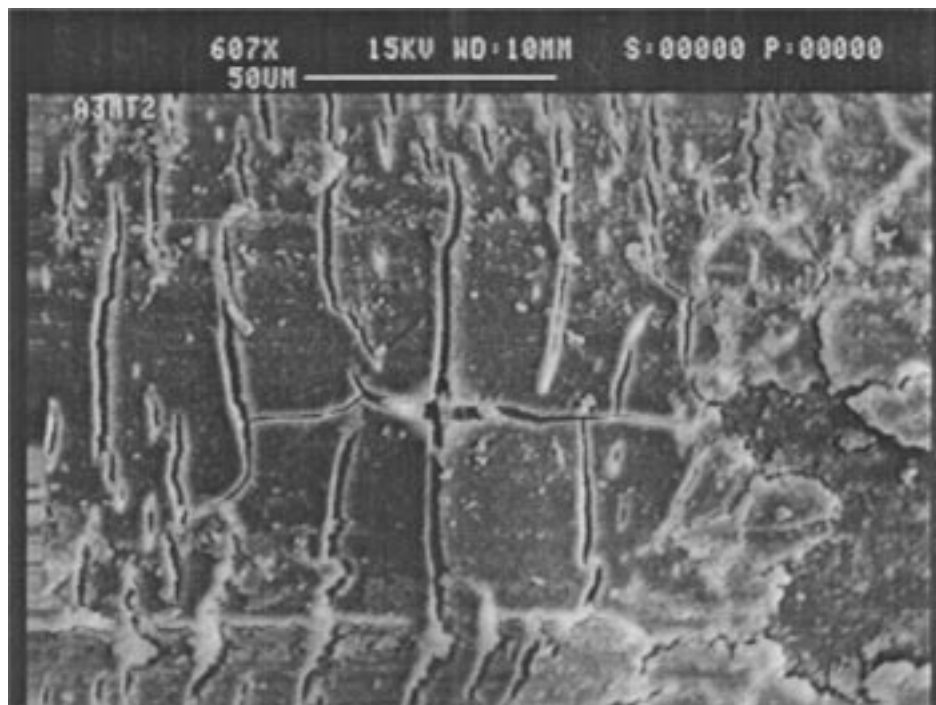
Before discussing how the pull-out test results are interpreted, it is important to review the principle of a few strain and crack sensors, and discuss how their performance may be affected by interfacial shear transfer.

The principles of two common strain sensors are illustrated in Fig. 11a and b. Fig. 11a shows the intrinsic

Fabry-Perot sensor [10]. The sensing part is a short length of fiber spliced to the end of a long fiber. When light is sent into the fiber, reflection occurs at both ends of the sensing part. By monitoring the interference between the two reflected signals, the elongation and strain in the sensing part can be obtained. Fig. 11b shows the Bragg grating sensor [5, 11]. A Bragg grating is a periodic variation of refractive index introduced along the optical fiber. When a broad-band light (i.e., light containing a wide spectrum of wavelengths) is sent through the fiber, the wavelength corresponding to the grating period will be preferentially reflected, resulting



(a)



(b)

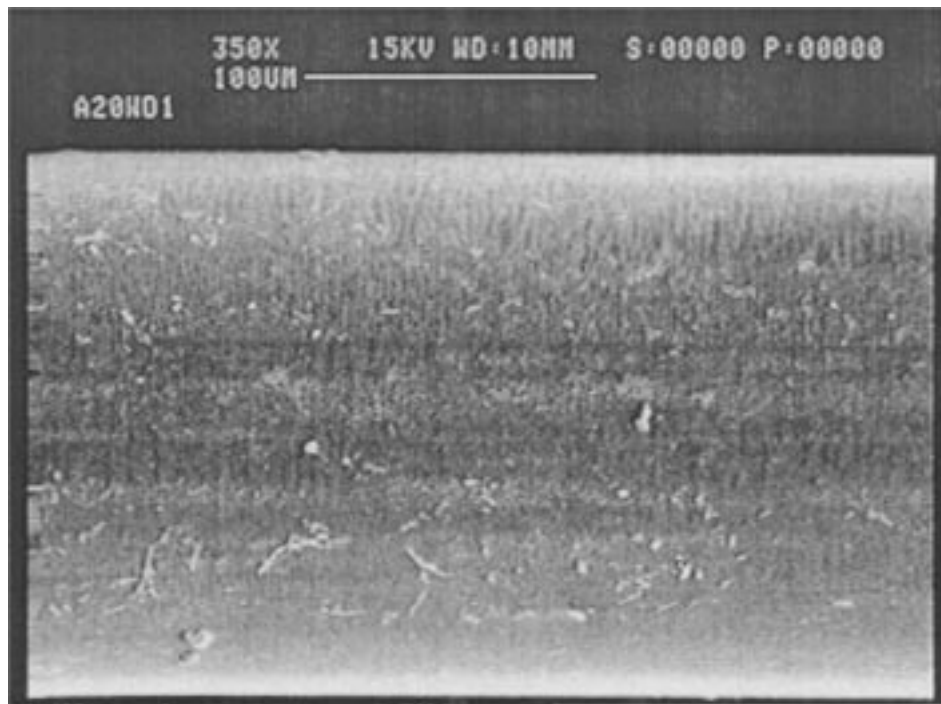
Figure 7 Acrylate-coated fiber in cement mortar for (a) three months (319 \times); (b) three months (607 \times).

in a peak wavelength in the reflected signal. When the grating is under strain, its length and hence its period will change. By monitoring the shift in the peak wavelength, the strain at the grating can be deduced.

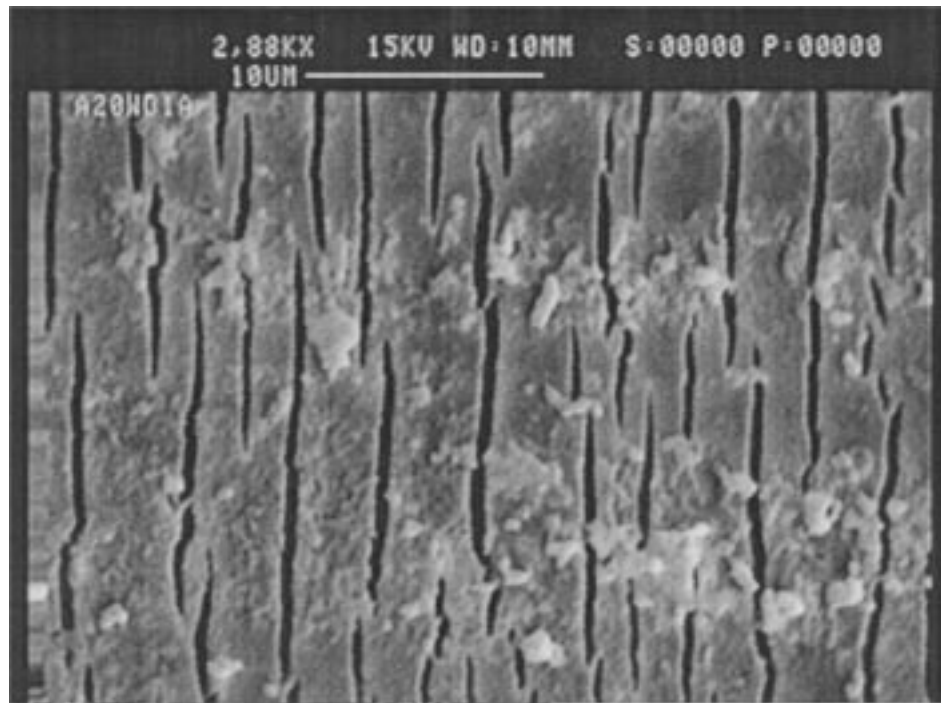
When tensile loading is applied to concrete, stress is transferred to the fiber through interfacial shear. Fig. 12a and b show the distributions of axial strain and interfacial shear stress along the fiber both before and after the occurrence of interfacial debonding. Before debonding, elastic behaviour governs and the fiber strain and interfacial shear stresses increases with the concrete strain in a self-similar manner. That is, if the

concrete strain is doubled, the shear stress and axial strain at any point along the fiber is also doubled. The fiber axial strain starts from zero at the fiber end, and reaches a steady state value (equal to the concrete strain) at a distance l_s into the fiber. After debonding, the interfacial shear stress distribution is no longer self-similar. Also, since debonding often leads to a reduction in shear transfer capability, the distance l_s has to increase.

Based on the change in strain distribution along the fiber, the consequence of debonding on strain sensing can be studied. For the Fabry-Perot sensor, what is measured is the average strain over the sensing part. This



(a)



(b)

Figure 8 Acrylate-coated fiber after 20 wetting/drying cycles (a) (350 \times); (b) (2880 \times).

average strain value is below the steady state strain and their ratio is the calibration factor of the sensor. As long as debonding has not started, this calibration factor is constant. Once debonding starts, the change in axial strain distribution (see Fig. 12a and b) will result in a change in average strain and shift in calibration factor. For the Bragg grating sensor, as long as it is at a distance $l > l_s$ from the fiber tip, the steady state strain (or strain in the concrete) will be measured. However, if excessive debonding leads to a significant increase in l_s , the calibration of the Bragg grating sensor will also be affected once debonding gets close to the location of the grating.

Besides strain sensing, embedded optical fibers can be employed for crack detection and monitoring (Ansari *et al.* [12], Leung *et al.* [6]). An example of such a sensor [6] is shown in Fig. 13. An inclined optical fiber is embedded in the concrete. As the crack opens, if the fiber is not bonded strongly to the concrete, it will slide and bend to stay continuous (see Fig. 13). Fiber bending will cause light to refract out of the fiber, and hence introducing a signal loss [11]. By monitoring the backscattered signal with Optical Time Domain Reflectometry (OTDR), the crack location and opening can be obtained from the time and magnitude of the drop. If several cracks are existing, the signal

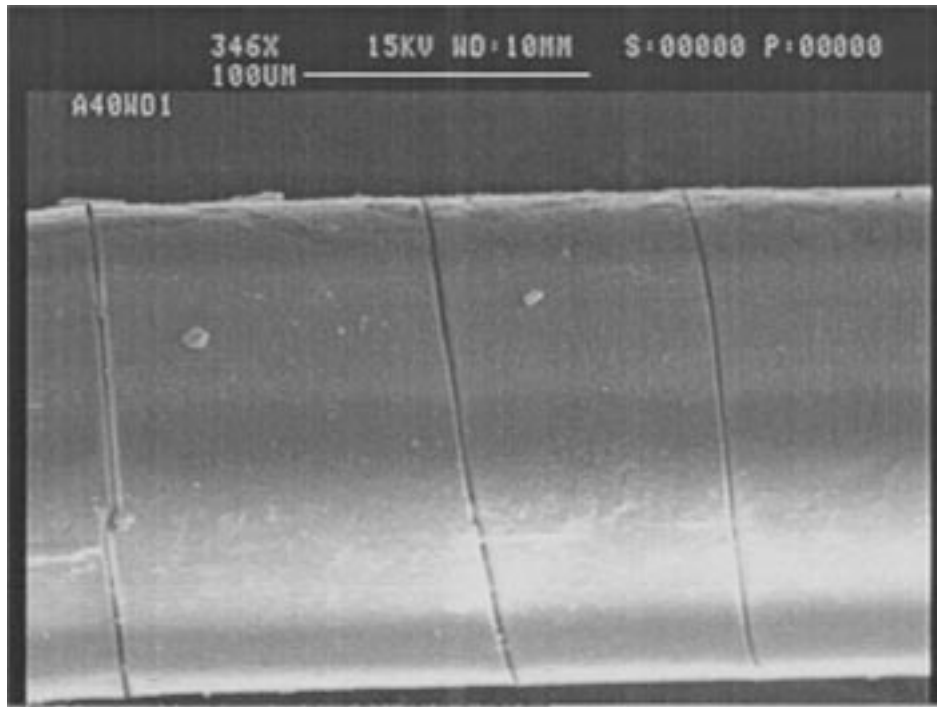


Figure 9 Acrylate-coated fiber after 40 wetting/drying cycles (346×).

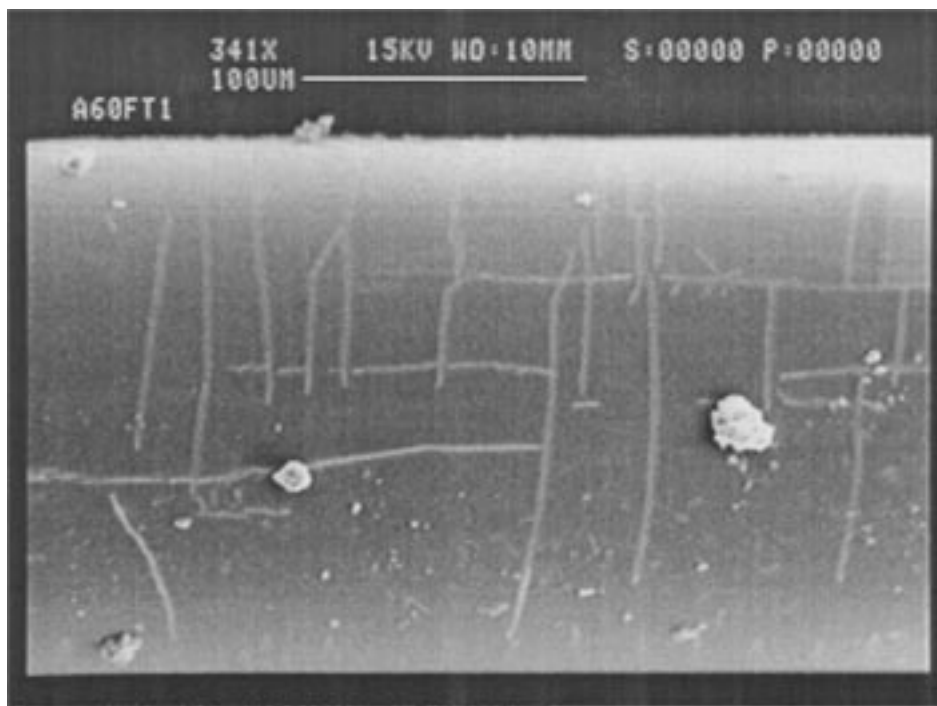


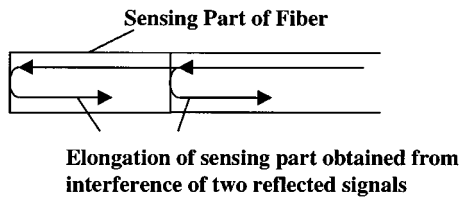
Figure 10 Acrylate-coated fiber after 60 freezing/thawing cycles (341×).

will exhibit a few drops. With this sensor, no a-priori knowledge of crack location is required. Also, it is possible to detect and monitor a number of cracks with one single fiber. For such a sensor to work, the fiber needs to be able to slide freely at the crack. A low interfacial shear transfer capability is desirable. If environmental exposure leads to a significant increase in interfacial shear capacity, the fiber may break at the crack at a very small opening. In such a case, the sensor can still tell the crack location (because significant backscattering can be observed at the broken end), but cannot serve the purpose of monitoring the crack opening. Also, it

is not possible to detect more than one crack with the fiber.

The interfacial shear transfer capability can be resulted from chemical bond, mechanical interlock or friction. To fully characterize this capability, several parameters are often required. In the literature, various approaches [7, 12–16] have been proposed for the determination of interfacial parameters from the pull-out record, and this is by no means trivial. Also, even if the interfacial parameters are known, the complete quantification of sensor behaviour (e.g., determining the relation between concrete strain and l_s , or, finding the

(a) Intrinsic Fabry-Perot Sensor



(b) Bragg Grating Sensor

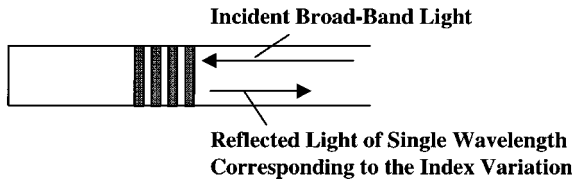
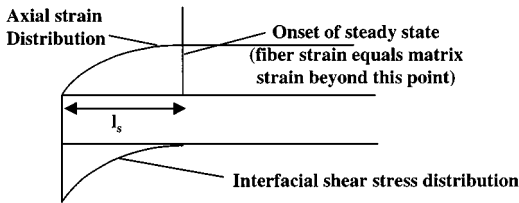


Figure 11 Two common types of optical fiber strain sensor.

(a) Strain Transfer before Debonding



(b) Effect of Interfacial Debonding on Strain Transfer

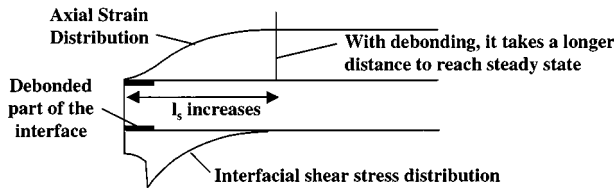


Figure 12 Effect of interfacial debonding on strain transfer to the optical fiber.

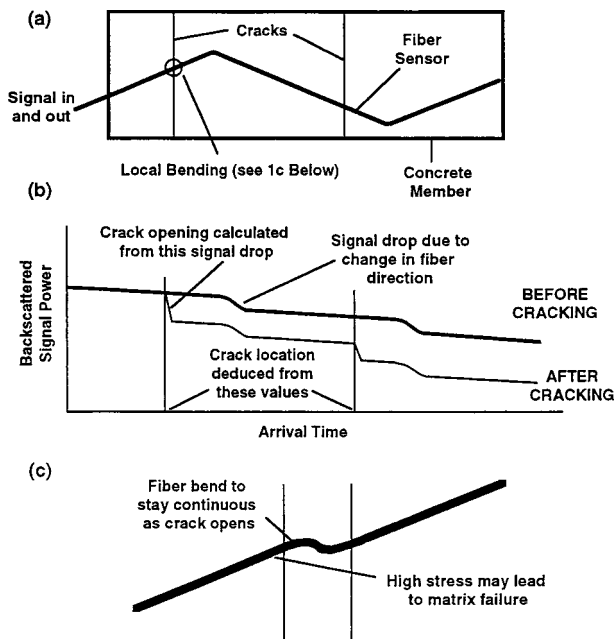


Figure 13 A novel crack sensing concept proposed by Leung *et al.* [6].

crack opening when breakage of optical fiber occurs) requires significant computation. In this work, as a first attempt to study the effect of environmental exposure on interfacial behaviour, our objective is not to quantify the sensor behaviour. Instead, we try to provide answers to the following questions. First, does the interfacial behaviour change significantly under a given environmental condition? Second, if the interface indeed changes, is it easier or more difficult for debonding to occur? By studying these two issues, we can determine whether a given environmental exposure is likely to affect strain sensing or crack sensing. For our purpose, we believe the simplest approach is to look at the change in peak load of the pull-out curve. It is obvious that the peak load itself is not sufficient to describe the complete pull-out behaviour. However, for a fixed fiber type and embedded length, the change in peak pull-out load under different environmental conditions does reflect how the interfacial shear capacity changes. In the following, we will therefore report the peak pull-out load for each test as the result of our study.

The results from the pull-out tests are given in Figs 14–16. In each figure, we show the maximum pull-out load after each kind of environmental exposure. Each figure consists of two plots. The upper one, denoted by (a), shows the results for all successful tests. To better observe the experimental trend, the average for each case is also plotted in (b). The results show that the different coatings behave very differently under the various environments. Embedment in moist mortar for three months does not affect the average peak pull-out

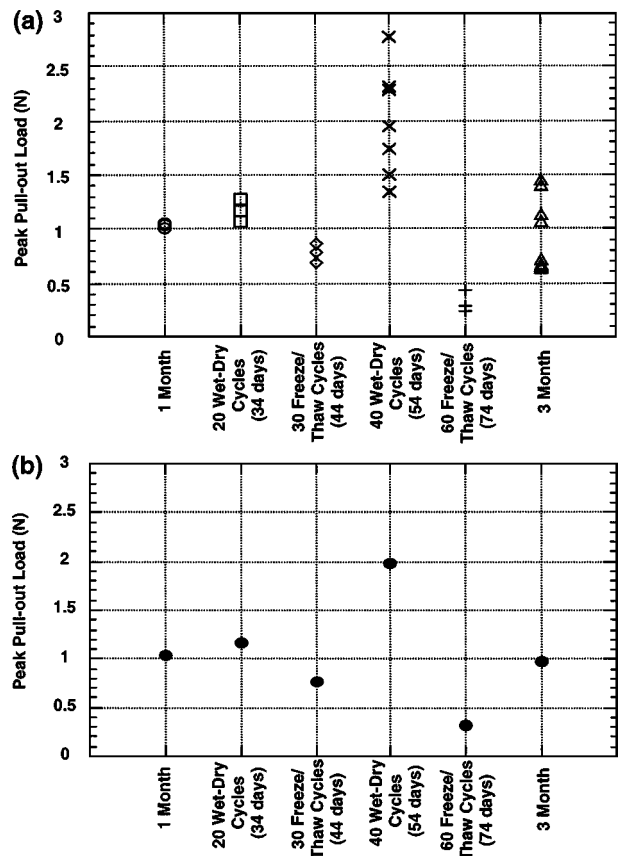


Figure 14 Peak pull-out load of acrylate coated fiber. (a) Results from all successful tests, (b) Average for each case.

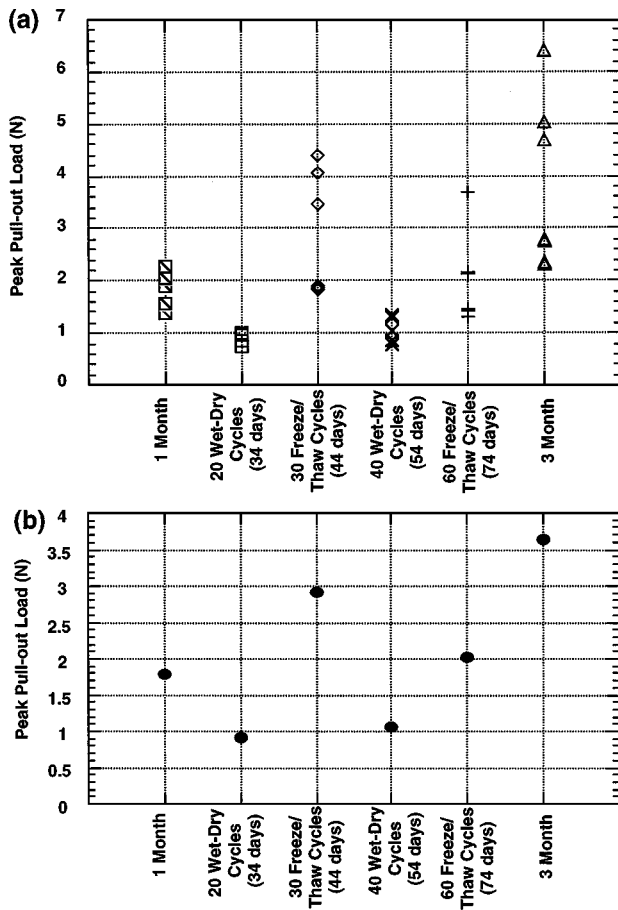


Figure 15 Peak pull-out load of polyimide/hytrel coated fiber. (a) Results from all successful tests, (b) Average for each case.

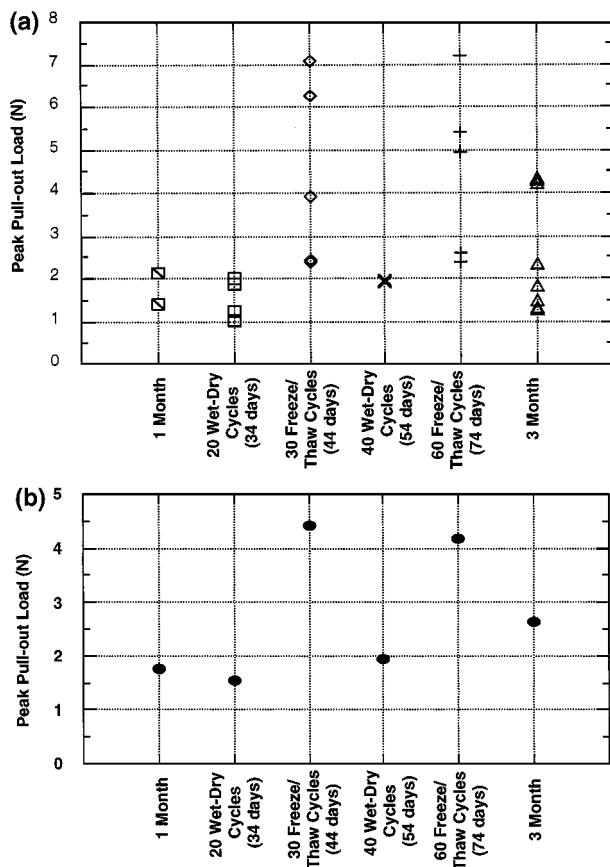


Figure 16 Peak pull-out load of teftzel-silicone coated fiber. (a) Results from all successful tests, (b) Average for each case.

load for acrylate coated fibers, although the variability does increase. For the polyimide coated fiber, however, three month embedment causes the peak pull-out load to double. For teftzel-silicone coated fiber, there is some increase in peak pull-out load after wet curing for 3 months. After 40 wet-dry cycles, the peak pull-out load for the acrylate coated fiber is doubled compared with specimens cured in mortar for a month. On the other hand, wetting and drying has little effect on the teftzel-silicone coating and decreases the peak pull-out load for polyimide coated fiber. Opposite effects of freeze/thaw cycles can also be observed for the various fibers. Freeze/thaw is found to decrease the peak pull-out load for the acrylate coated fiber, while significantly increasing the interfacial resistance for the teftzel-silicone fiber. For the polyimide fiber, the peak pull-out load increases a lot after 30 freeze/thaw cycles but decreases from 30 to 60 cycles. Actually, a slight decrease in peak pull-out load from 30 to 60 freeze/thaw cycle can also be observed for the teftzel-silicone coated fiber. The exact reason is not understood at this point.

In summary, different precautions should be taken for different applications and different fiber coatings. For strain sensing, we should be careful about freezing/thawing for acrylate fibers, and wetting/drying for polyimide fibers. Teftzel-silicone fibers appear to have no problem. This is consistent with the findings in [9], where optical fiber strain sensors with teftzel-silicone coatings are found to perform well after 5-year embedment in concrete. For crack sensing, if polyimide is used, the structure should be kept dry as exposure to water results in the highest increase in peak pull-out load. For acrylate, wetting/drying is to be avoided, and for teftzel-silicone, freezing/thawing should be prevented.

It is interesting to note that the fiber pull-out test is much more sensitive to changes than the SEM examination described above. In many cases where the SEM study cannot reveal any changes, the maximum pull-out load shows significant differences. The present investigation therefore demonstrates that time dependent interfacial behavior of embedded optical fiber sensors can be properly assessed with the fiber pull-out test. SEM examination, however, serves a complementary role. For example, when significant changes in the pull-out behaviour has been obtained, it is important to carry out SEM examination as well. If the interfacial changes are found to be due to the cracking or deterioration of the protective coating, alkaline ions may start to penetrate the coating and attack the glass fiber. In this case, even if the stress transfer condition is still satisfactory after interfacial changes occur, the possibility of chemical attack on the glass fiber should not be overlooked.

4. Conclusion

In this investigation, changes at the optical fiber/concrete interface under various environmental conditions have been studied with both scanning electron microscopy and the fiber pull-out test. In particular, a fiber pull-out testing procedure has been developed for the study of interfacial changes in optical fibers. Experiments are carried out with three types of fiber coating

(acrylate, polyimide/hytrel, teftzel-silicone) under various environmental conditions (curing in water, wetting/drying, freezing/thawing). The results show that the fiber pull-out test can reveal significant changes in interfacial behaviour that cannot be detected from SEM examination. The pull-out test is therefore demonstrated to be a useful technique for the characterization of time dependent interfacial behavior for embedded optical fiber sensors. It should be performed as a first test to study interfacial changes. If the pull-out test reveals significant changes, SEM investigation should then be carried out to see if there is excessive coating degradation that may lead to chemical attack on the glass fiber.

References

1. W. R. HABEL, D. HOFMANN and D. HOFMANN, in Proceedings of Second European Conference on Smart Structures and Materials, Glasgow, October 1994, edited by A. McDonach *et al.*, p.180.
2. D. R. HUSTON, P. FUHR, P. J. KAJENSKI, T. P. AMBROSE and W. B. SPILLMAN, in Proceedings of First European Conference on Smart Structures and Materials, Glasgow, May 1992, edited by B. Culshaw *et al.*, p. 409.
3. A. HOLST and W. HABEL, *ibid.* p. 223.
4. R. MAASKANT, T. ALAVIE, R. M. MEASURES, G. TADROS and S. H. RIZKALLA, *Cem. & Conc. Comp.* **19** (1996) 21.
5. M. A. DAVIS, D. G. BELLEMORE and A. D. KERSEY, *ibid.* **19** (1996) 45.
6. C. K. Y. LEUNG, N. ELVIN, N. OLSON, T. F. MORSE and Y.-F. HE, *Engrg. Fract. Mech.* **65** (2000) 133.
7. Z. LI, B. MOBASHER and S. P. SHAH, *J. Am. Ceram. Soc.* **74** (1991) 2156.
8. W. R. HABEL and H. POLSTER, *IEEE J. of Ltwave. Tech.* **13** (1995) 1324.
9. P. ESCOBER, V. GUSMEROLI, M. MARTINELLI, I. LANCIANI and P. MORABITO, in Proceedings of First European Conference on Smart Structures and Materials, Glasgow, May 1992, edited by B. Culshaw *et al.*, p. 215.
10. T. YOSHINO, K. KUROSAWA, K. ITOH and T. OSE, *IEEE J. Quant. Elect.* **QE-18** (1982) 1624.
11. G. R. MELTZ, W. W. MOREY and W. H. GLEN, *Opt. Lett.* **18** (1993) 1370.
12. F. ANSARI and R. K. NAVALURKAR, *ASCE J. Eng. Mech.* **119** (1993) 1048.
13. P. BARTOS, *J. Mat. Sci.* **15** (1980) 3122.
14. Y. GAO, Y. W. MAI and B. COTTERELL, *J. Appl. Math. Phys. (ZAMP)* **39** (1988) 550.
15. C. K. Y. LEUNG and V. C. LI, *Comp.* **21** (1990) 305.
16. A. E. NAAMAN, G. C. NAMUR, J. M. ALWAN and H. NAJM, *ASCE J. Eng. Mech.* **117** (1991) 2791.

*Received 12 April 1999
and accepted 22 May 2000*